NASA TECHNICAL NOTE

NASA TN D-3612

NASA TN D-3612

C. 1

WIND-TUNNEL INVESTIGATION OF THERMAL AND PRESSURE ENVIRONMENTS IN THE BASE OF THE SATURN S-IC BOOSTER FROM MACH 0.1 TO 3.5

by Robert A. Wasko

Lewis Research Center

Cleveland, Ohio

NATIONAL AERONAUTICS AND SPACE ADMINISTRATION • WASHINGTON, D. C. • SEPTEMBER 1966

WIND-TUNNEL INVESTIGATION OF THERMAL AND PRESSURE ENVIRONMENTS IN THE BASE OF THE SATURN S-IC BOOSTER FROM MACH 0.1 TO 3.5

By Robert A. Wasko

Lewis Research Center
Cleveland, Ohio

NATIONAL AERONAUTICS AND SPACE ADMINISTRATION

For sale by the Clearinghouse for Federal Scientific and Technical Information
Springfield, Virginia 22151 – Price $1.00

WIND-TUNNEL INVESTIGATION OF THERMAL AND PRESSURE ENVIRONMENTS IN THE BASE OF THE SATURN S-1C BOOSTER FROM MACH 0.1 TO 3.5

by Robert A. Wasko

Lewis Research Center

SUMMARY

A 1/45 scale model of the Saturn S-1C booster was tested from Mach 0.1 to 3.5 and at altitudes from sea level to 150 000 feet in order to examine trends in convective and radiative heating rates and in pressures in the base region as affected by model geometric variations such as engine shroud length, introduction of cooling air into the base, and nozzle gimbal angle. The effects of a nonoperating center engine were also determined.

Results indicate that trends in convective and radiative heating agree with predicted trends. Convection reached a maximum at transonic Mach numbers and low altitudes and decreased to low values at supersonic Mach numbers and high altitudes, whereas radiation was maximum near sea level and decreased with increasing altitude.

Changes in model geometry tended to decrease heating rates from values obtained for the configuration with the longest shroud and without base-cooling-air devices. However, at high altitudes, a shorter shroud increased heating as did certain nozzle-gimbal patterns. Maximum convective heating rates tended to occur at a base location between the outboard nozzles, while radiation reached a maximum further outboard. Base pressure was less than free-stream static pressure and was nearly constant across the base at altitudes to 36 000 feet. At higher altitudes, it was greater than ambient and decreased in magnitude from the inner to the outer region of the base. Shortening the shroud increased base pressure to 36 000 feet but decreased it at higher altitudes. Cooling-air scoops and deflectors increased base pressure at altitudes less than 66 000 feet but decreased it at higher altitudes. A nonoperating center engine resulted in a slight change in base pressure at low altitudes but a decrease at high altitudes, whereas nozzle gimbal decreased base pressure over the entire trajectory.

INTRODUCTION

The thermal and pressure environments in the base of rocket-powered vehicles must be adequately defined if an optimum design is to be realized. Base heating results from the circulation of hot gases into the base, radiation from the jet afterburning plume, and in some cases burning of combustible gases entrained in the base.

Scale-model tests are used to study these phenomena, but as discussed in reference 1, it is not presently possible to design a model that provides a rigorous simulation of the full-scale base environment. Important parameters that may be suitably simulated include the vehicle trajectory and geometry, in addition to engine chamber pressure, oxidant-to-fuel ratio, combustion efficiency, and nozzle geometry. Parameters not suitably controlled are the jet-exit temperature profile and a multiplicity of factors affecting the external combustion phenomenon (jet afterburning and base burning of entrained fuel). An additional complication is that of scaling the model heating rates to full-scale values. At present, this scaling is based on simple theories or empirical relations that provide some degree of success provided that the base-burning phenomenon is not a significant effect with either the model or the flight vehicle (ref. 2). The value of model tests, therefore, lies in studying trends with test variables. It is expected that the data are useful for preliminary design purposes, but it is important that accurate flight measurements of the full-scale base thermal environment be obtained as quickly as possible in the development of a launch vehicle.

A 1/45 scale model of the Saturn S-1C was tested in the Lewis 8- by 6-foot transonic wind tunnel and the 10- by 10-foot supersonic wind tunnel at free-stream Mach numbers from 0.1 to 3.5 and altitudes from sea level to 150 000 feet. The program was conducted to examine the convective and radiative heating rates and pressures in the base region with variations in engine shroud length, introduction of cooling air into the base, a nonoperating engine, and operation with the engines gimbaled.

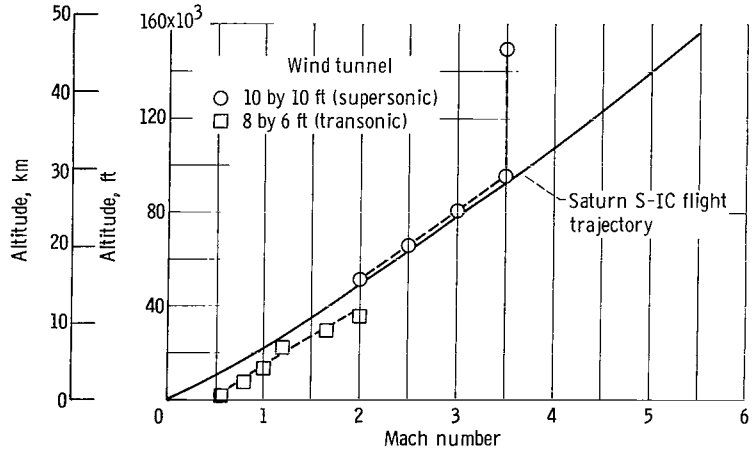

Figure 1. - Comparison of flight and model trajectory.

SYMBOLS

O/F	oxidant-fuel ratio
$\overline{p}_b$	average base pressure
p_0	free-stream static pressure
q_c	convective heating rate, W/cm^2 or $Btu/(ft^2)(sec)$
q_r	radiative heating rate, W/cm^2 or $Btu/(ft^2)(sec)$
R	radius of model base, 4.4 in.
r	radial position on base plate, in.
θ	angular position on base plate measured from vertical, deg

APPARATUS AND PROCEDURE

The variation of altitude with free-stream Mach number is shown in figure 1 for both the 8- by 6-foot transonic wind tunnel and the 10- by 10-foot supersonic wind tunnel test conditions. Also shown is a flight trajectory, typical of the Saturn S-1C. The 8- by 6-foot-tunnel altitude simulation was limited by the facility to a lower trajectory than flight, but the 10- by 10-foot-tunnel test conditions were controlled to duplicate the flight trajectory to an altitude of 96 000 feet. Although the test conditions at 150 000 feet occurred at too low a Mach, the free-stream Mach number has a relatively minor effect on the base environment at this high altitude.

The model was 8.8 inches in diameter and 148 inches long and was installed in the 8- by 6-foot transonic wind tunnel as shown in figure 2. Only the afterbody was a 1/45 scale of the S-1C geometry. (Ref. 3 describes full-scale geometry and propulsion system details.) The model length was dictated by a shock-tube combustor specially designed by the Cornell Aeronautical Laboratory. A schematic drawing of the combustor is shown in figure 3 and is described in reference 4 (which also discusses the use of the short-duration technique in base-heating studies). Essentially, the operation of the combustor is as follows: Ethylene and gaseous oxygen were used to simulate the full-scale propellants, kerosene and liquid oxygen, and were pumped into long charge tubes within the model. The ethylene was stored at 2100 pounds per square inch absolute and the gaseous oxygen at 2400 pounds per square inch absolute. A fast-acting valve permitted these gases to flow simultaneously from their respective charge tubes, through an injector, and into a combustion chamber. Spark ignition produced constant-pressure combustion for about 20 milliseconds simulating the nominal full-scale F-1 chamber pressure of 1100 pounds per square inch absolute at an O/F ratio of 2.25. The gases were manifolded to five nozzles with F-1 engine contours and area ratios of 16.

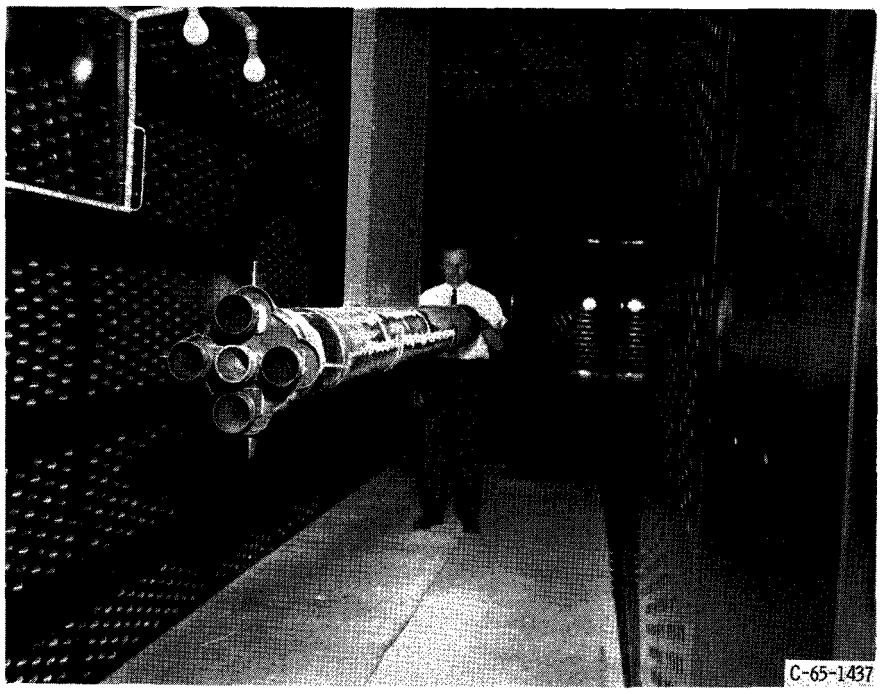

Figure 2. - Saturn S-IC model installation in 8- by 6-foot tunnel.

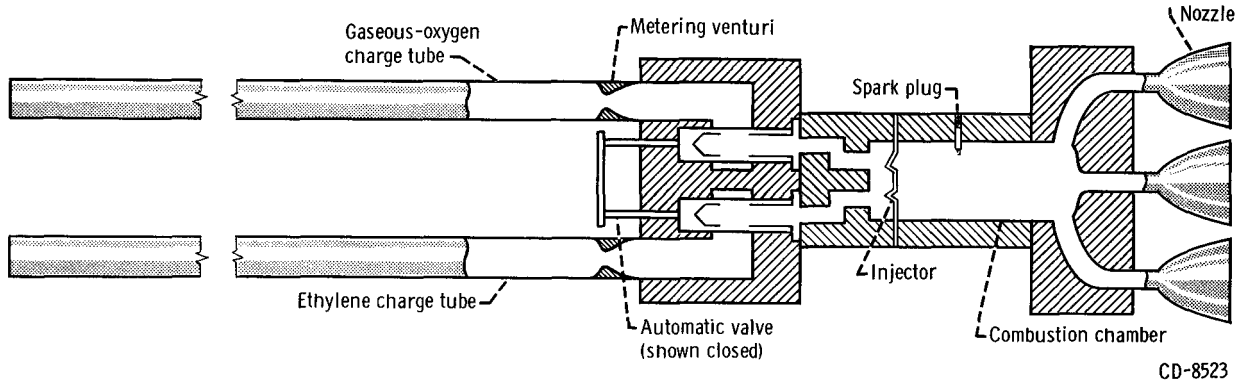

Figure 3. - Schematic drawing of shock-tube combustor.

The ethylene charge tube was unheated during the 10- by 10-foot-tunnel test; however, a possibility existed for two-phase flow to occur between the charge tube and combustion chamber. Therefore, this charge tube was heated to 250° F during the 8- by 6-foot-tunnel test to ensure a more precise control of the O/F ratio.

Turbine exhaust gases were introduced into the nozzle through circumferential holes simulating the F-1 engine exhausterator. Figure 4 compares the full-scale and model engine geometries and shows the external ducting of the exhausterator to the nozzle. Turbine exhaust effects were simulated with both hydrogen and ethylene. Hydrogen was used because its wide flammability limits might be expected to cause a more severe base-

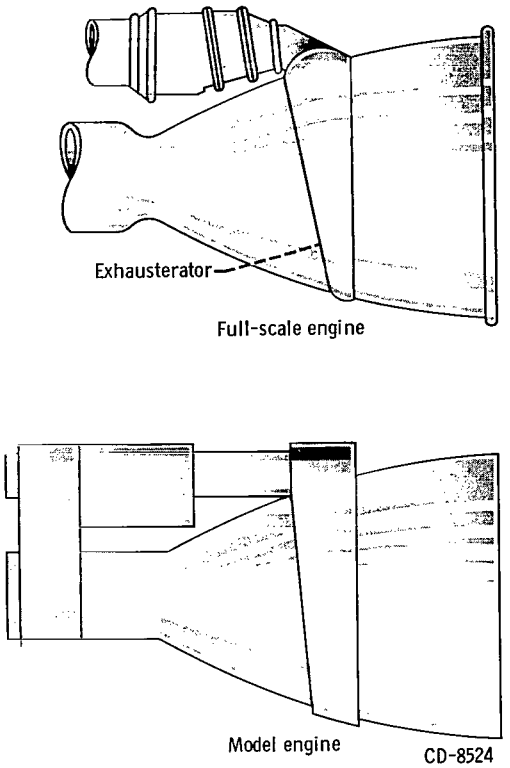

Figure 4. - Comparison of full-scale and model F-1 engine geometry.

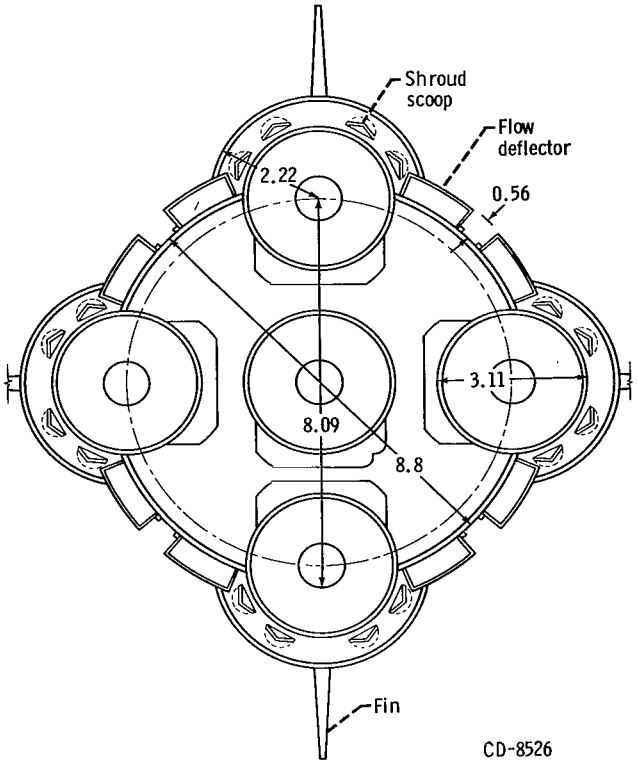

Figure 5. - Model base geometry. (All dimensions are in inches.)

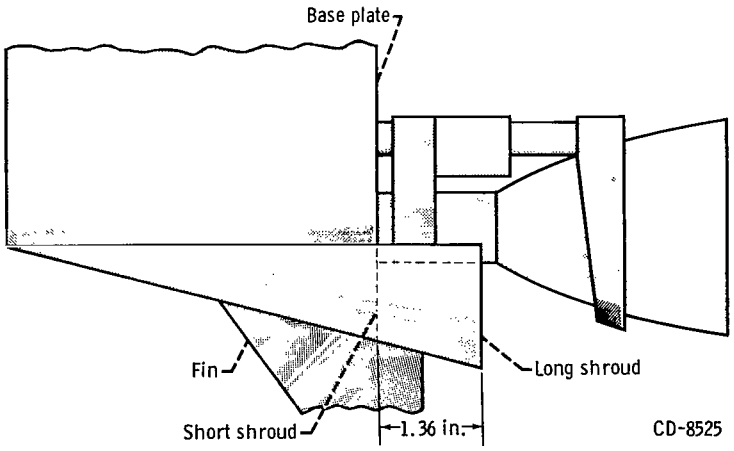

Figure 6. - Comparison of long and short engine shrouds.

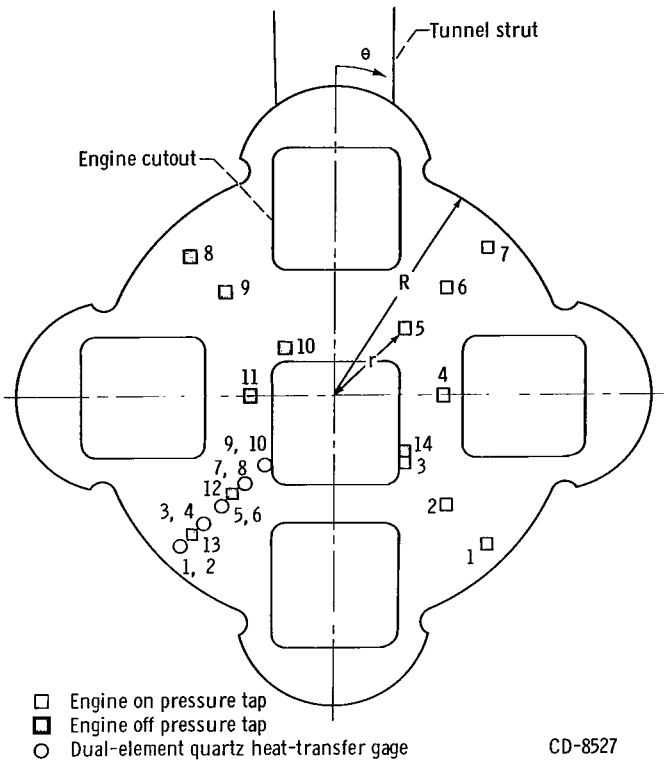

Figure 7. - Base-plate instrumentation layout. (Outer gages, odd numbered - total gages; inner gages, even numbered - radiant gages. See table I.)

heating condition and, hence, ensure that the model tests would lead to a conservative vehicle design. The ethylene was used because it is a hydrocarbon with similarities to kerosene in the fuel-rich turbine exhaust of the full-scale engine. The hydrogen weight flow was scaled on the basis of the heat release from combustion of the excess fuel in the full-scale turbine exhaust. This procedure has been used in previous base-heating tests, as described in reference 5. The ethylene weight flow was scaled to provide the same ratio of turbine-exhaust to nozzle weight flow as the full-scale engine.

Figure 5 shows base geometry details such as spacing dimensions, scoops, and deflectors for passage of cooling air into the base and the engine shrouds. Scoop and deflector heights, as well as base dimensions, are a 1/45 geometric scaling of full-scale values. Two engine shroud lengths were tested (fig. 6). The long shroud extended over each outboard engine 1.36 inches. The short shroud extended only to the base-plate station, as shown.

Details of base-plate instrumentation location are shown in figure 7 and table I. The base plate was water cooled so that a reference temperature of approximately 100° F could be maintained. Convective and radiant heating rates were obtained from thin-film calorimeters developed for shock-tube wink tunnels and are described in detail in references 6 and 7. The calorimeters were unique because convection and radiation rates could be obtained from the same gage by a dual-element system. A thin film of platinum deposited on the front of a quartz button gave a total heating rate to the surface obtained from the temperature variation of platinum film with time and heat-transfer theory (ref. 6). A film deposited on the back of the quartz gave the radiation component after appropriate corrections had been made for the optical properties of the quartz (ref. 7). Convection was obtained from the difference between total and radiation heating rates.

Piezoelectric pressure transducers were used to obtain jet-on base pressure and are described in reference 8. Pressure taps were used to sense jet-off base pressure at a given free-stream condition of altitude and Mach number prior to initiation of combustion.

TABLE I. - BASE-PLATE INSTRUMENTATION POSITIONS

[a]Instrument location	Component		Dimensionless position coordinate, r/R	Angular position on base plate, θ, deg
□	Engine on pressure tap	1	0.900	135
		2	.650	135
		3	.400	135
		4	.430	90
		5	.400	45
		6	.650	45
		7	.900	45
▩	Engine off pressure tap	8	0.848	315
		9	.638	315
		10	.277	315
		11	.342	270
		12	.588	225
		13	.837	225
		14	.350	129
○	Dual-element quartz heat-transfer gage	1, 2	0.900	225
		3, 4	.775	225
		5, 6	.650	225
		7, 8	.525	225
		9, 10	.400	225

[a]See fig. 7.

Since the piezoelectric transducers registered only a change in pressure from jet-off values, the sum of the jet-off and the transducer pressures yielded jet-on values.

Traces of pressure variation with time and heat flux were observed on oscilloscopes and recorded in photographs taken during the test event. The cameras were mounted directly on the oscilloscopes and timed with the combustor firing sequence (ref. 8).

RESULTS

Base Heating

Base-plate distribution. - Figure 8 shows a typical radial distribution of heating rates in the base. The configuration consisted of the long shroud, no-cooling-air devices, and hydrogen turbine exhaust gas. Convection and radiation rates are plotted as a function of a nondimensionalized position coordinate. The symbols identify free-stream Mach number and altitude.

At altitudes to 36 000 feet, convective heating was maximum between the outboard engines (r/R = 0.65) but at higher altitudes, the distribution was more nearly uniform. At low altitudes, radiation rates reached a maximum further outboard than the convection rates, and the maximum occurred at r/R = 0.775. However, above 36 000 feet, the level was constant across the base and near zero.

General trends and turbine exhaust effect. - Heating rates for the long-shroud configuration without cooling-air devices are shown in figure 9(a). Gage 3, 4 located at r/R = 0.775 was chosen for this and succeeding comparisons (except as noted), since it was near the location of the maximum heating rates as shown in figure 8.

Model convective heating increased sharply from sea level (Mach 0.1) to a maximum that occurred at an altitude of 8000 feet (Mach 0.8) and then decreased sharply to low values at high altitudes. Radiation heating rates varied in an erratic manner with free-

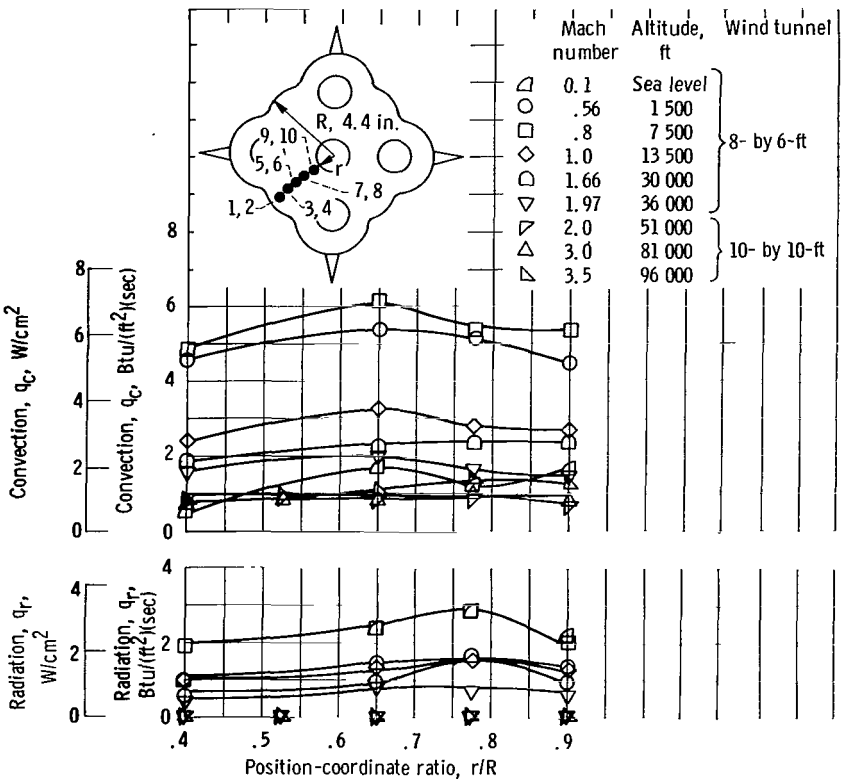

Figure 8. - Typical base-plate heat-transfer distribution. Long shroud; no-cooling-air configuration; hydrogen turbine exhaust.

stream conditions, but the trend of the data shows a decrease in radiation with increasing altitude from a sea-level maximum.

The 10- by 10-foot-tunnel test was conducted prior to the 8- by 6-foot-tunnel test. During the program in the 10- by 10-foot tunnel, it was found that the use of the unheated ethylene charge tube did not ensure a precise control of the O/F at 2.25. However, since the heating rates appeared to vary in a systematic manner and were consistent with the 8- by 6-foot tunnel results wherein proper O/F control was maintained, they are assumed valid. The base-pressure data presented in another section is similarly valid because O/F variation does not produce a significant effect on base pressure.

A large effect of turbine exhaust gas on convection can be seen in figure 9(a), whereas effects on radiation rates were not clearly defined. Maximum convective values recorded were 3.6 Btu per square foot per second for no turbine exhaust, 5.4 for hydrogen, and 9.2 for ethylene. A possible cause for this increase with turbine exhaust flow may be the combustion of turbine exhaust gas in the boundary of the exhaust jet ahead of the jet free-stream interaction zone, thereby increasing the temperature of the recirculated gases above the no-turbine-exhaust case. Another possible cause is a base-burning phenomenon wherein the combustible gases were entrained and burned within the base region.

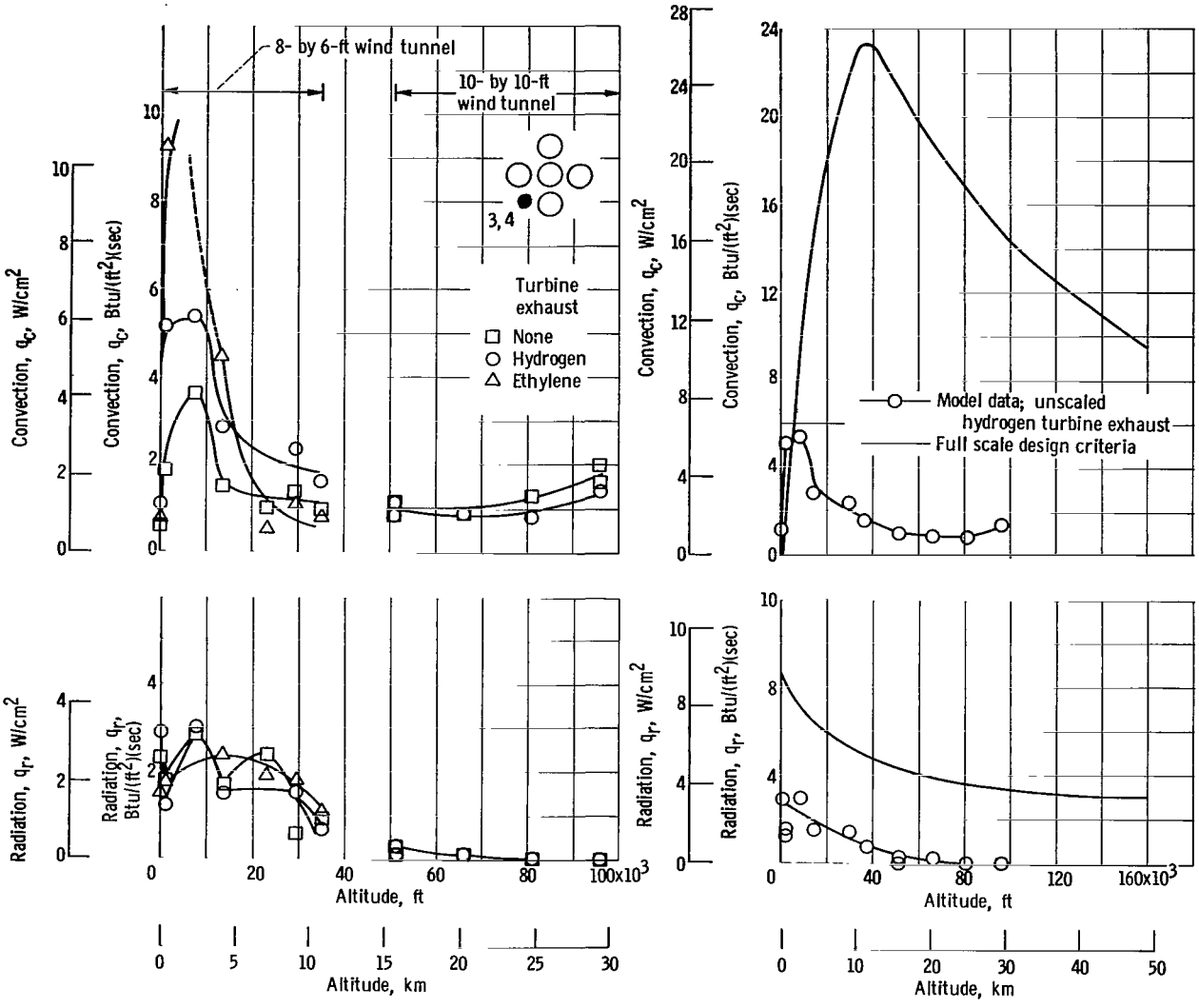

Figure 9. - General trends and turbine exhaust effects. Long shroud; no-cooling-air configuration.

In previous base-heating studies (ref. 1), this phenomenon was observed to be sporadic and intermittent and, therefore, is not amenable to an accurate analysis with this short-duration technique.

The higher convective heating rates obtained from the use of ethylene turbine exhaust (rather than hydrogen turbine exhaust) was an unexpected result. However, the higher values for ethylene are not entirely a result of the change in gas species. They are also related to the difficulty in timing the arrival of ethylene turbine exhaust gas with the combustion gases. Ethylene has a slower speed of sound than hydrogen with the result that hydrogen achieves steady flow conditions in the turbine exhaust ducting almost instantaneously, whereas ethylene has a slower transient rise to steady state. Therefore,

ethylene flow was initiated prior to the combustion gases so that ethylene achieved steady flow concurrent with the nozzle flow. During the transient period in ethylene flow, the base was filled with turbine exhaust gas. This situation could produce different mixing and reaction kinetics between turbine-exhaust and nozzle flow than would exist if the ethylene could arrive instantaneously. Consequently, it is believed that the ethylene heating rates are a gross consequence of a phenomenon related to the operation of this model and do not simulate flight conditions. In succeeding figures all comparisons will be made with hydrogen as the turbine-exhaust-gas simulator.

Estimates of full-scale Saturn S-1C convective and radiative base-heating rates are shown in figure 9(b). These curves were obtained from design criteria (ref. 9 and unpublished data from Marshal Space Flight Center) and are based on a wall reference temperature of 100° F, as are the model data, repeated from figure 9(a) for comparison purposes. Full-scale convective heating rates increased from sea level to a maximum that occurs near 37 000 feet (Mach 1.5) and decreased sharply at higher altitudes. Radiation predictions show a decrease in altitude from a sea-level maximum. It can be seen that the observed trends in model data agree with trends in full-scale predictions for both convection and radiation. Although scaling factors have not been applied to the model convective heating rates (since heat-transfer coefficients and recovery temperature were not obtained in this program), their application tends to decrease the anticipated value. Hence, the design criteria, when compared with model data obtained with this short-duration technique, represent a fairly conservative estimate.

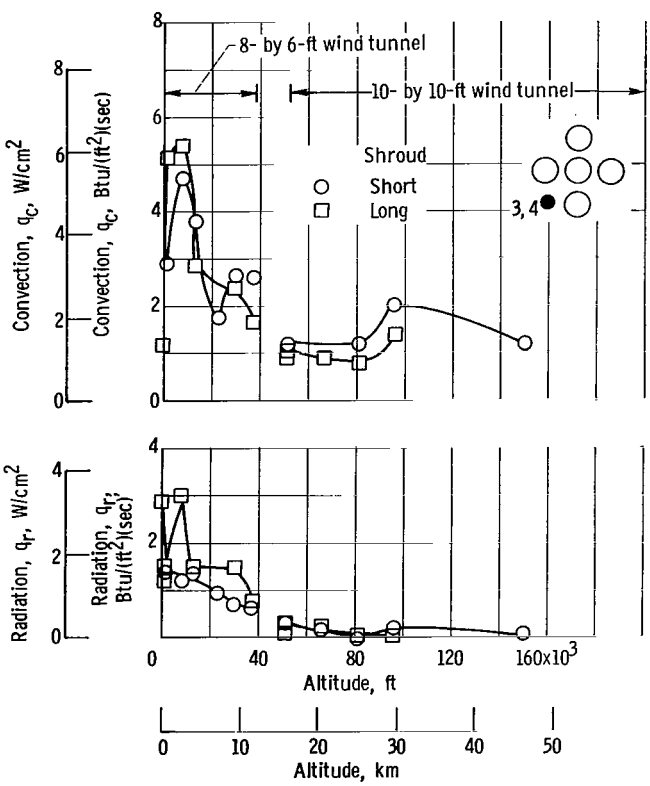

Figure 10. - Effect of shroud length on base heat transfer. No-cooling-air configuration; hydrogen turbine exhaust.

Effect of shroud length. - Heating rates for the long and short shrouds, without base-cooling-air devices, are compared in figure 10. Little difference was noted in convection at altitudes to 36 000 feet except at 1500 feet (Mach 0.56) where the long shroud had a value of 5.2 Btu per square foot per second compared with 2.9 for the short shroud. At higher altitudes, the values of convection for the short shroud were only slightly higher than those for the long

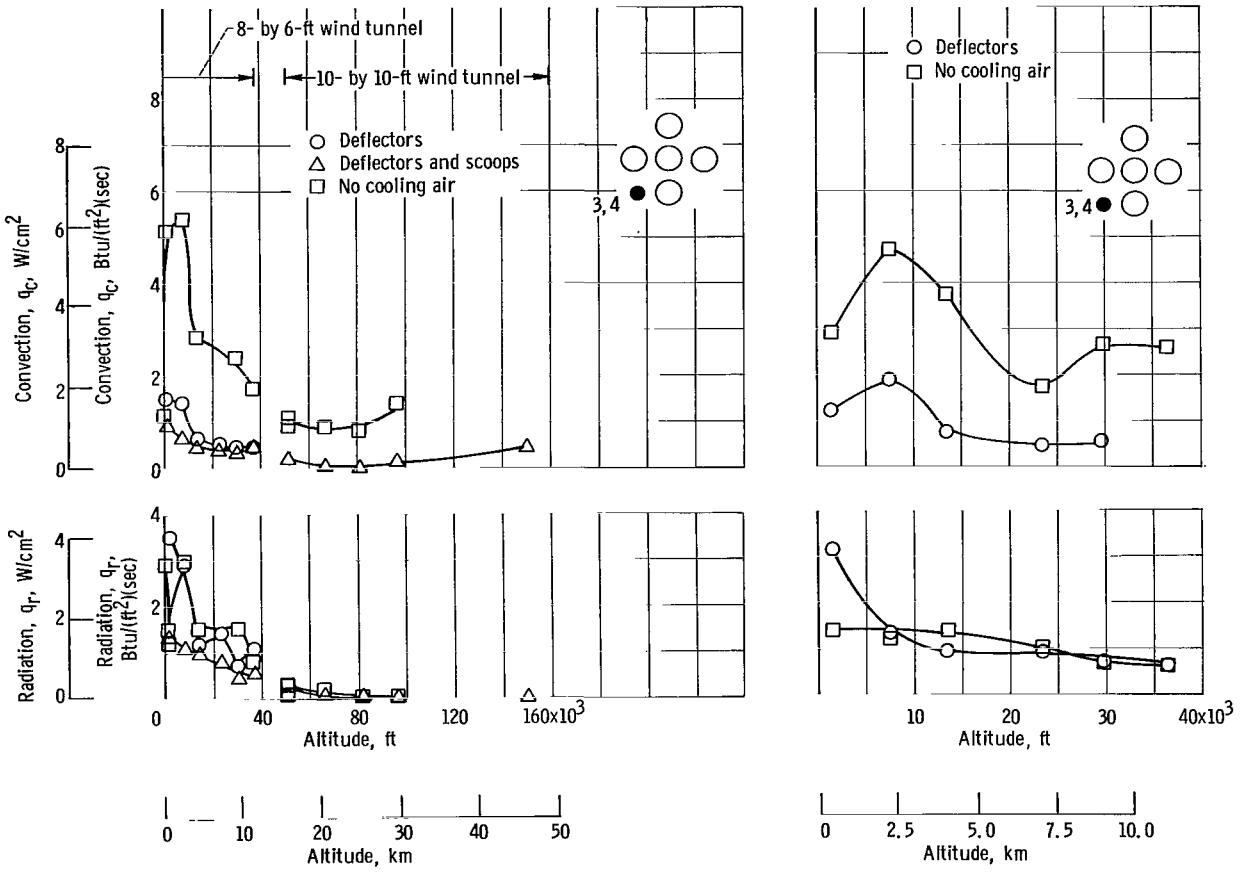

(a) Long shroud, hydrogen turbine exhaust.

(b) Short shroud; hydrogen turbine exhaust.

Figure 11. - Effect of cooling air on base heat transfer.

shroud. Radiative rates were erratically higher for the long shroud at altitudes to 36 000 feet and were nearly zero at higher altitudes for both configurations.

Effect of cooling air. - Figure 11(a) shows the effect of cooling air, introduced into the base through scoops and/or deflectors, for the long-shroud configuration. Convective heating rates were reduced significantly with the use of these cooling-air devices over the entire trajectory. At altitudes to 36 000 feet, maximum convective heating was reduced nearly 75 percent by their use, and at higher altitudes convective heating was almost eliminated. Scoops plus deflectors reduced convective heating only slightly below that achieved with the deflectors alone. In general, cooling air also decreased the radiation at altitudes to 36 000 feet, but this decrease was not as signficant as that for convection. At higher altitudes, effects on radiation were not observed since the radiation level was low.

The effect of cooling air with the short-shroud configuration was obtained only in the 8- by 6-foot tunnel and results are shown in figure 11(b). As observed for the long-shroud configuration, cooling air significantly decreased the convective heating rates; however, little effect was seen on radiative rates except at 1500 feet where the introduction of cooling air caused an increase.

Effect of nonoperating engine. - Figure 12 shows the effect of a nonoperating center engine on base heat transfer. This engine was chosen because it would produce

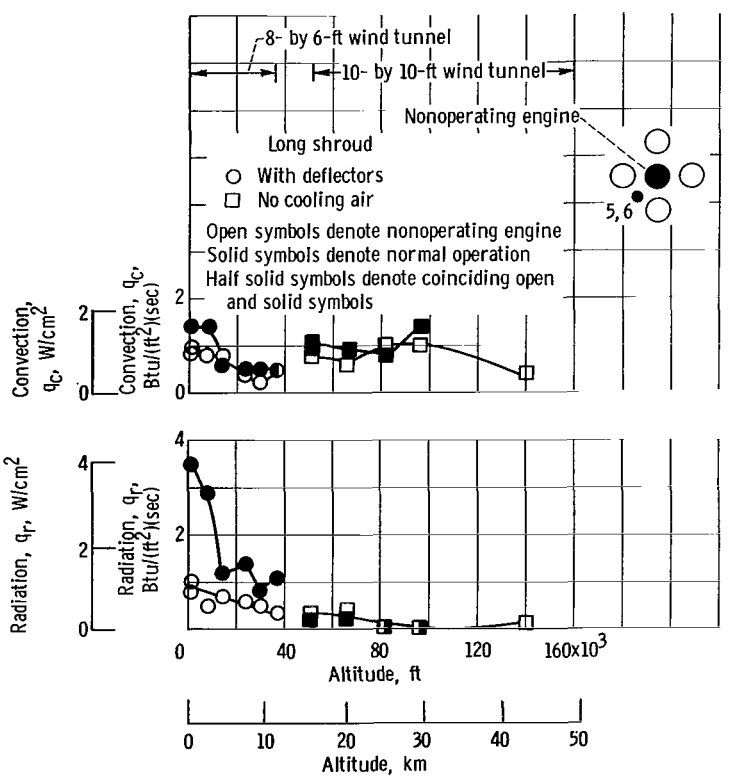

Figure 12. - Effect of nonoperating engine on base-heat transfer. Hydrogen turbine exhaust.

the most significant effect on base heating, since the flow from the center engine interacts with flow from all other nozzles. Gage 5, 6 was used for this particular comparison because of instrumentation difficulties with gage 3, 4. The data from the 8- by 6-foot tunnel are for the long-shroud-plus-deflector configuration, whereas the 10- by 10-foot data are for the long shroud with no-cooling-air configuration. Since a significant effect of cooling air on base heating has been previously noted, data for these configurations cannot be compared directly. Rather, these results are intended to show qualitatively the effect of a nonoperating engine at low and high altitudes. At low altitudes, a slight reduction in convection was noticed at altitudes less than 13 500 feet (Mach 1.0), while radiation was reduced at all altitudes tested (e.g., from 3.5 to 1.0 Btu/ft^2 sec at 1500 ft, Mach 0.56). At high altitudes, the heating rates were essentially unchanged.

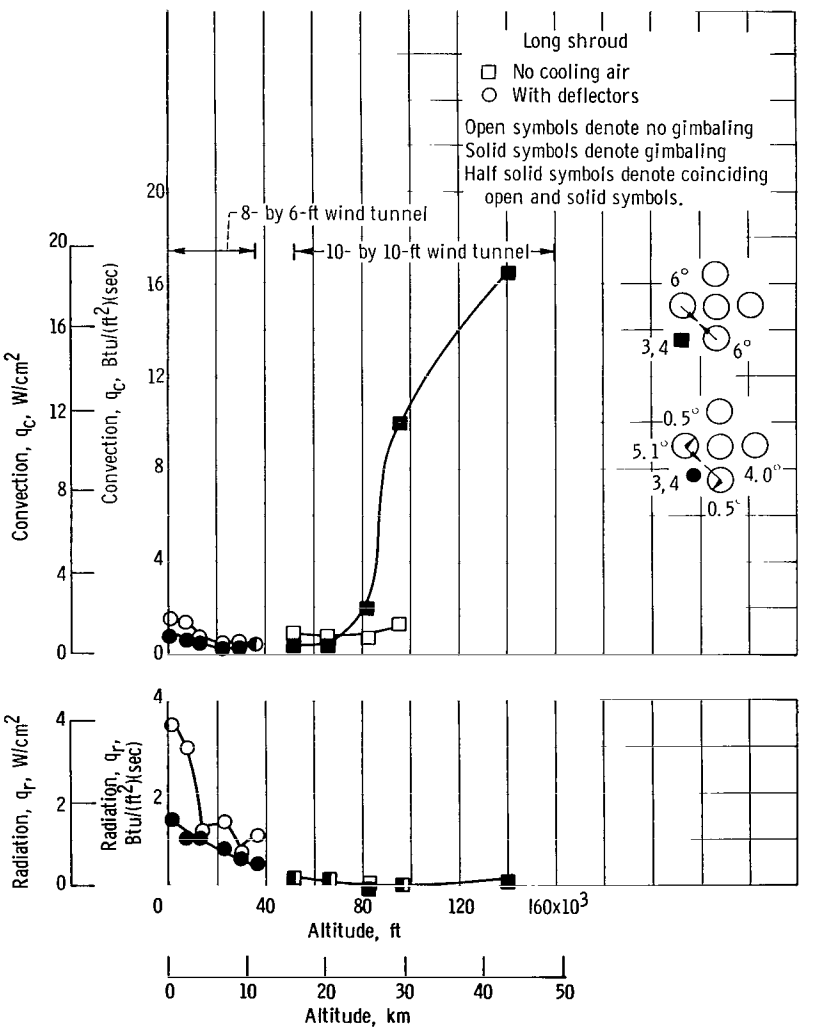

Figure 13. - Effect of nozzle gimbal on base heat transfer. Hydrogen turbine exhaust.

Effect of nozzle gimbal. - The effect of nozzle gimbal is shown in figure 13. As was the case with a nonoperating engine, the long-shroud configuration with deflectors was utilized for the 8- by 6-foot-tunnel data, and the long-shroud no-cooling-air configuration was used for the 10- by 10-foot-tunnel data. Furthermore, the gimbal pattern was different for each configuration, as shown in the key. Yet, each gimbal pattern has a significant amount of gimbal in the direction of adjacent nozzles to increase the impingement of these jets. These data are intended to show the effect of this increased jet interaction both at low and at high altitudes. At most of the low altitudes, a reduction in convection and radiation occurred, particularly at altitudes less than 13 500 feet (Mach 1. 0). At high altitudes, no effect was seen on radiation, but convection was slightly reduced at altitudes to 66 000 feet (Mach 2. 5) and thereafter increased rapidly to values as high as 16 Btu per square foot per second at 150 000 feet. This indicates that, at high altitudes, convective base heating can be significantly affected by gimbal patterns that increase the jet impingement.

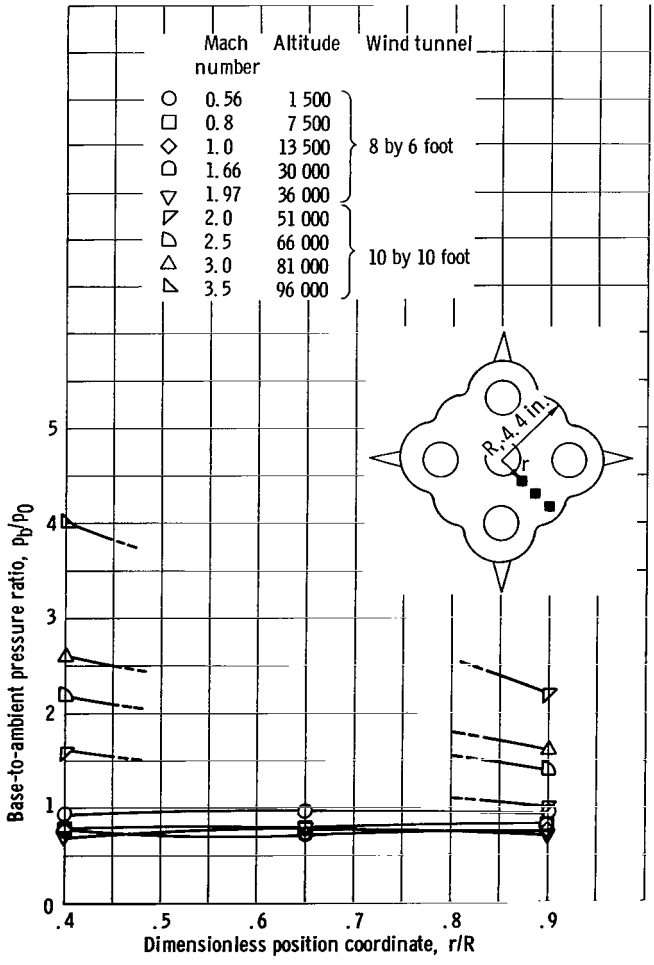

Figure 14. - Base-plate pressure distribution. Long shroud; no cooling-air configuration; hydrogen turbine exhaust.

Base Pressure

Base pressures are shown in figures 14 to 18, and hydrogen turbine exhaust flow was used for all data presented. Comparisons with similar data without turbine exhaust indicate the absence of an effect.

Base-plate distribution. - A typical distribution of base pressures is shown in figure 14 for the long-shroud no-cooling-air configuration. Base-to-ambient pressure ratio is plotted as a function of the dimensionless position coordinate r/R. Pressures were uniform across the base at altitudes to 36 000 feet. At higher altitudes, the base pressure decreased from the inner to the outer regions of the base in a manner undefined because of the lack of data.

Effect of shroud length. - In figure 15 and succeeding figures, an average base to free-stream static-pressure

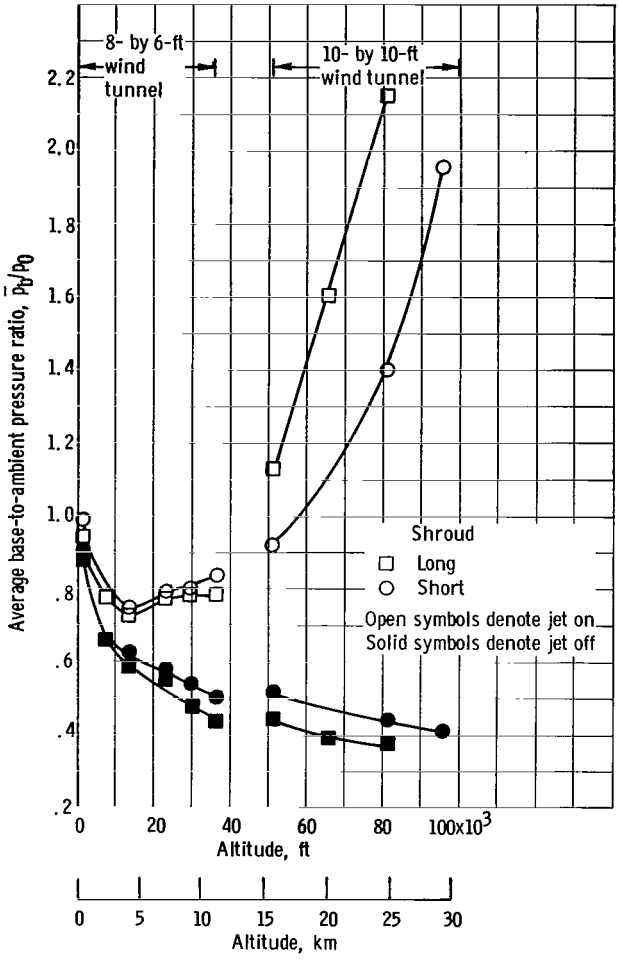

Figure 15. - Effect of shroud length on base pressure. No-cooling-air configuration.

ratio is plotted as a function of altitude. Jet-on base pressures for the short shroud were greater than base pressures for the long shroud at altitudes to 36 000 feet, but were less at higher altitudes. At altitudes to 36 000 feet, the long-shroud base was aspirated ($p_b/p_0 < 1.0$), whereas the short-shroud base was aspirated to 60 000 feet. Jet-off base pressure was less for the long shroud in both the 8- by 6-foot and 10- by 10-foot tunnels except at altitudes less than 13 000 feet where shroud length had no effect. Jet-on base pressure was always greater than jet-off base pressure.

A detailed discussion of flow in the base of rocket-powered vehicles is presented in reference 10. In the light of that discussion, some general comments may be made on these trends of the base-pressure data. By referring to figure 15, it is seen that, as altitude increases, the jet-off base pressure decreases, which is normally observed for an axisymmetric body with a blunt base. At altitudes to 13 500 feet (Mach 1.0), jet-on base-pressure ratio also decreased with increasing altitude. However, as altitude increases, the jet expansion and interaction with the free stream produces a stronger recirculation of flow into the base. Consequently, the jet-off and jet-on curves diverge. For altitudes above 13 500 feet, the base-pressure ratio increases with altitude and the base eventually becomes pressurized. At very high altitudes, the jets are fully impinged, and the base is primarily affected by mutual jet interactions rather than free-stream effects.

An unexpected result was observed at altitudes less than 13 500 feet. At these altitudes the jets are over expanded and would not produce base recirculation. Rather, the jets should act as an ejector pump and reduce base pressures from jet-off values. However, the opposite trend was observed in the data. This may have been influenced by a possible tunnel flow phenomenon in that the extreme length of the model dictated locating the afterbody near the end of the perforated test section, a region of local flow acceleration (and reduced static pressure) at Mach numbers less than 1.0. In fact, a comparison of these base pressures to unpublished data from a cold flow model of the S-1C tested in the 8×6 indicated poor agreement. At these same conditions, jet-off base pressures were

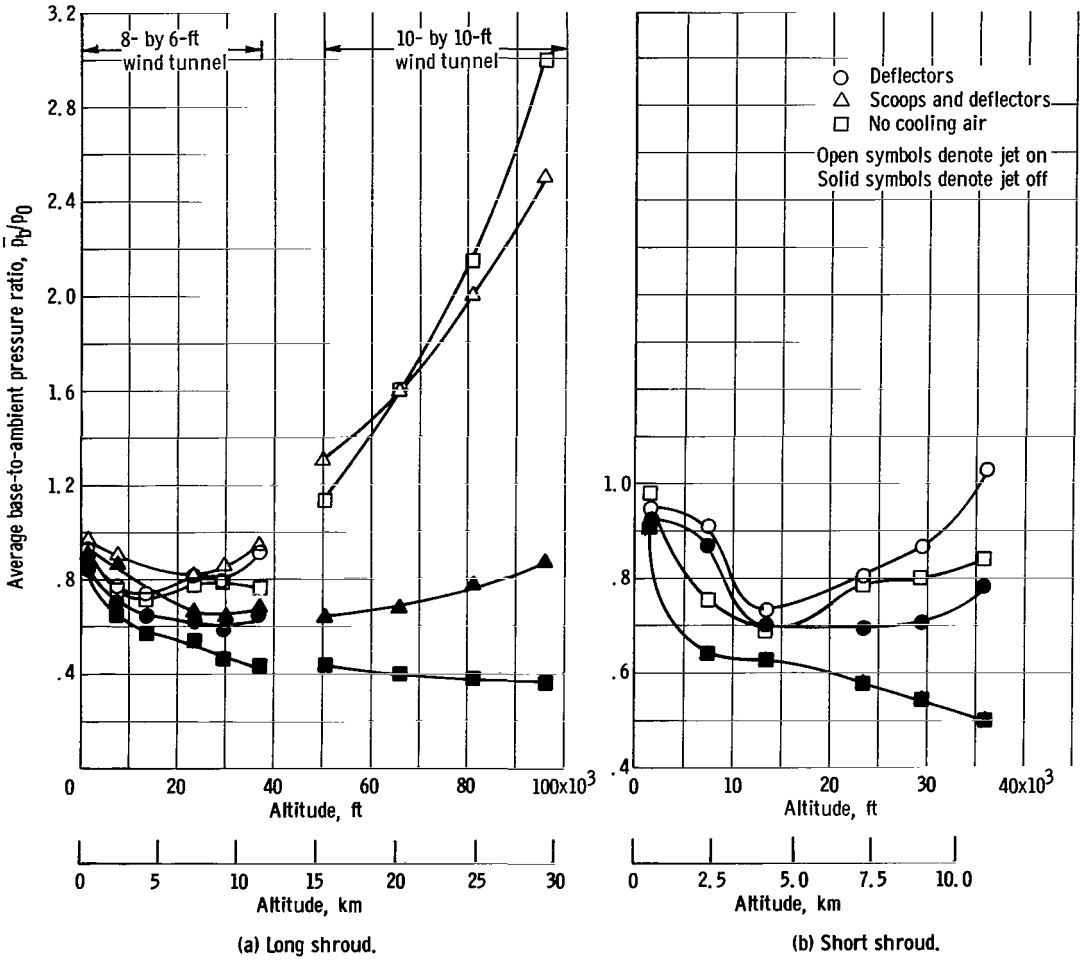

Figure 16. - Effect of cooling air on base pressure.

greater than those presented herein and jet-on base pressures were less than jet off as would be expected. However, the cold flow model was located such that its afterbody was not in this accelerated flow field.

Effect of cooling air. - Data for the long-shroud configuration (fig. 16(a)) indicated that at altitudes to 66 000 feet, jet-on pressures were greater for the scoop and/or deflector configurations except at 1500 feet where there was little effect. Because more air was brought into the base with scoops and deflectors than with deflectors alone, the base pressure was greater for the configuration with scoops and deflectors. Above 66 000 feet, jet-on base pressure was less for the cooling-air configuration. This fact may be a result of reverse flow from the base through the scoops and deflectors, since the base is highly pressurized at these altitudes.

The short-shroud configuration (fig. 16(b)) was tested only in the 8- by 6-foot tunnel, and the effects of cooling air were similar to those for the long shroud, except at 1500 feet where the base pressures were slightly reduced with deflectors. Jet-off base pressure was greater with cooling-air devices for both configurations over the entire trajectory.

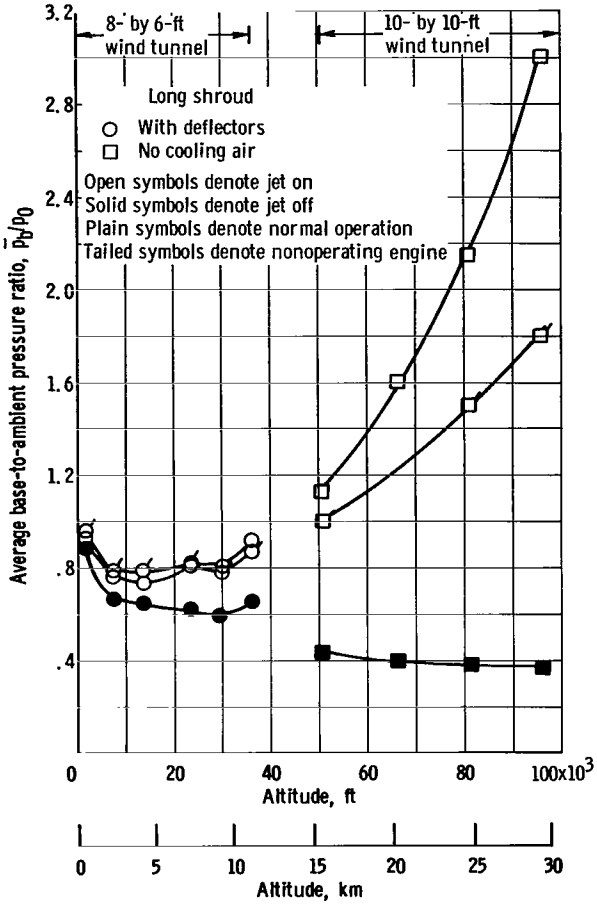

Figure 17. - Effect of engine out on base pressure.

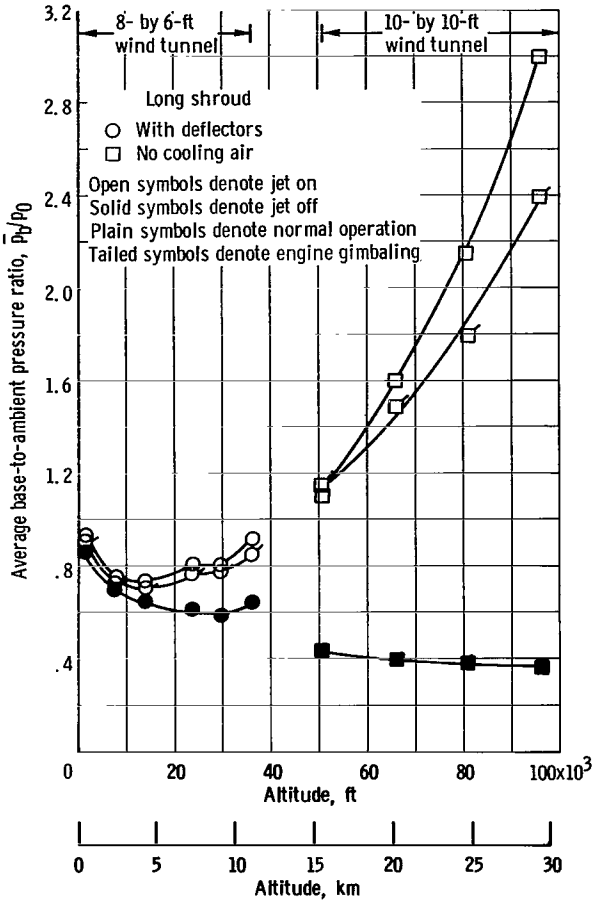

Figure 18. - Effect of nozzle gimbal on base pressure.

Effect of nonoperating engine. - Figure 17 shows the effect of a nonoperating center engine on base pressure. The 8- by 6-foot-tunnel configuration had the long shroud and deflectors, whereas the 10- by 10-foot-tunnel configuration did not have deflectors. As shown in figure 16, deflectors do not change base pressure to any great extent; therefore, the data from both tunnels are compared directly.

The base pressure with a nonoperating center engine was slightly greater than the pressure during normal operation to 24 000 feet, but it was less thereafter. These trends indicate that a nonoperating center engine reduces base pressures at those altitudes of jet impingement and/or base pressurization. In effect, the amount of mass recirculated by jet impingement is reduced.

Effect of nozzle gimbal. - Shown in figure 18 is the nozzle-gimbal effect for gimbal patterns and configurations that are identical to those shown in figure 13 (p. 13). In general, these gimbal patterns produced a slight reduction in the base pressure at low altitudes and a significant reduction at higher altitudes.

SUMMARY OF RESULTS

A 1/45 scale model of the Saturn S-1C was tested from Mach 0.1 to 3.5 and altitudes from sea level to 150 000 feet in order to study the base heating and pressure environment as affected by geometric variables such as engine shroud length, introduction of cooling air into the base, and nozzle gimbal angle. The effects of a nonoperating center engine were also investigated. The following results were obtained for base heating:

1. The trend of convective and radiative heating rates agree with predicted trends in that convection reached a maximum at the transonic Mach numbers and low altitudes and decreased to low values at supersonic Mach numbers and high altitudes; radiation was maximum at altitudes near sea level.

2. Turbine exhaust gas increased convective heating rates. Maximum values recorded were 3.6 Btu per square foot per second for no turbine exhaust, 5.4 for hydrogen, and 9.2 for ethylene. Radiation varied erratically with turbine exhaust but the maximum value that was observed was 3.5 Btu per square foot per second.

3. Maximum heating occurred on the long-shroud no-cooling-air configuration. Generally, changes in the model geometry and operation with a nonoperating center engine decreased these heating rates. However, at high altitudes, shortening the shroud produced slightly higher convective heating, and gimbal patterns that increase jet impingement significantly increased convection.

4. At altitudes to 36 000 feet, convective heating rates were maximum at a location between the outboard nozzles, but at higher altitudes the distribution across the base was uniform. Radiant heating was maximum at a point further outboard from that for convection at altitudes to 36 000 feet; however, at higher altitudes the radiation rates were near zero.

The following results were obtained for base pressures:

1. Generally, base pressure was less than free-stream static pressure to 36 000 feet, but greater thereafter.

2. Pressures were nearly constant across the base at altitudes to 36 000 feet and decreased from the inner to the outer regions of the base at higher altitudes.

3. Shortening the shroud increased base pressure to 36 000 feet but decreased base pressure at higher altitudes.

4. Introduction of cooling air into the base by scoops and deflectors increased base pressure at altitudes less than 66 000 feet but decreased base pressure at higher altitudes.

5. A nonoperating center engine resulted in little base-pressure change at low altitudes and decreased base pressure at the higher altitudes where the jets impinged and the base was pressurized.

6. Nozzle gimbal produced lower base pressures over the entire trajectory, with the largest effect at high altitudes.

Lewis Research Center,
National Aeronautics and Space Administration,
Cleveland, Ohio, May 5, 1966.

REFERENCES

1. Beheim, Milton A.; and Obery, Leonard J.: Wind Tunnel Studies of Booster Base Heating. Astronautics and Aero-Space Eng., vol. 1, no. 1, Feb. 1963, pp. 111-117.

2. Jones, Ira P., Jr.: Summary of Base Thermal Environment Measurements on the Saturn 1 Block 1 Flight Vehicles. NASA TM X-53326, 1965.

3. Kovit, Bernard: The Saturns. Space/Aeronautics, vol. 42, no. 2, Aug. 1964, pp. 40-52.

4. Hendershot, K. C.: The Application of Short-Duration Techniques to the Experimental Study of Base Heating. Rep. No. HM-1510-Y-18, Cornell Aeronautical Lab., Inc., Apr. 1965.

5. Allen, John L.; and Wasko, Robert A.: Base Heat Transfer, Pressure Ratios, and Configuration Effects Obtained on a 1/27 Scale Saturn (C-1) Model at Mach Numbers from 0.1 to 2.0. NASA TN D-1566, 1963.

6. Vidal, Robert J.: Transient Surface Temperature Measurements. Rep. No. CAL-114, Cornell Aeronautical Lab., Inc., Mar. 1962.

7. Bogdan, Leonard: Measurement of Radiative Heat Transfer With Thin Film Resistance Thermometers. Rep. No. HM-1510-4-9 (NASA CR-57125), Cornell Aeronautical Lab., Inc., July 1963.

8. Martin, James F.; Duryea, George R.; and Stevenson, Leroy M.: Instrumentation for Force and Pressure Measurements in a Hypersonic Shock Tunnel. Rep. No. 113, Cornell Aeronautical Lab., Inc., Jan. 1962.

9. Mullen, C. R.: Analysis of Saturn S-IC Base Heating Environment. Rep. No. D5-11287, Boeing Co., Sept. 1964.

10. Goethert, B. H.; and Barnes, L. T.: Some Studies of the Flow Pattern at the Base of Missles with Rocket Exhaust Jets. Rep. No. AEDC TR 58-12, Arnold Engineering Development Center, June 1960.

"The aeronautical and space activities of the United States shall be conducted so as to contribute . . . to the expansion of human knowledge of phenomena in the atmosphere and space. The Administration shall provide for the widest practicable and appropriate dissemination of information concerning its activities and the results thereof."

—NATIONAL AERONAUTICS AND SPACE ACT OF 1958

NASA SCIENTIFIC AND TECHNICAL PUBLICATIONS

TECHNICAL REPORTS: Scientific and technical information considered important, complete, and a lasting contribution to existing knowledge.

TECHNICAL NOTES: Information less broad in scope but nevertheless of importance as a contribution to existing knowledge.

TECHNICAL MEMORANDUMS: Information receiving limited distribution because of preliminary data, security classification, or other reasons.

CONTRACTOR REPORTS: Technical information generated in connection with a NASA contract or grant and released under NASA auspices.

TECHNICAL TRANSLATIONS: Information published in a foreign language considered to merit NASA distribution in English.

TECHNICAL REPRINTS: Information derived from NASA activities and initially published in the form of journal articles.

SPECIAL PUBLICATIONS: Information derived from or of value to NASA activities but not necessarily reporting the results of individual NASA-programmed scientific efforts. Publications include conference proceedings, monographs, data compilations, handbooks, sourcebooks, and special bibliographies.

Details on the availability of these publications may be obtained from:

SCIENTIFIC AND TECHNICAL INFORMATION DIVISION

NATIONAL AERONAUTICS AND SPACE ADMINISTRATION

Washington, D.C. 20546